A MEASUREMENT OF $\sin^2\theta_W$ FROM THE FORWARD–BACKWARD ASYMMETRY IN $p\bar{p} \to Z^0 \to e^+e^-$ INTERACTIONS AT $\sqrt{s} = 1.8$ TeV

BY

PETER TODD HURST

B.S., Massachusetts Institute of Technology, 1985
M.S., University of Illinois, 1986

THESIS

Submitted in partial fulfillment of the requirements
for the degree of Doctor of Philosophy in Physics
in the Graduate College of the
University of Illinois at Urbana-Champaign, 1990

Urbana, Illinois

List of Tables

4.1 Tight CEM electron quality cuts. 45

4.2 Electron quality requirements for the second electron in a Z^0 event. 45

4.3 Efficiencies for individual electron quality parameters determined from the W and Z^0 data samples. 57

4.4 Electron isolation efficiencies. 59

5.1 Results of the various parameter determinations after background corrections 81

5.2 Mean and sigma of fits to multiple toy Monte Carlo data samples 82

5.3 Mean and sigma of the distribution of the differences between fits to the toy Monte Carlo data samples. 83

5.4 Log likelihood fit results for various parton distribution function parametrizations 95

5.5 Systematic uncertainties on A_{FB} and $\sin^2\theta_W$. 95

A.1 Vector and axial vector components and corrected propagators used in the weak corrections to $q\bar{q} \to e^+e^-$. 136

List of Figures

2.1 Feynman diagram for inverse muon decay, $e^-\bar{\nu}_e \to \mu^-\bar{\nu}_\mu$. 7

2.2 Momenta and spins in inverse muon decay, $e^-\bar{\nu}_e \to \mu^-\bar{\nu}_\mu$. A single arrow indicates the direction of a particle's momentum vector, while the double arrow shows the projection of the particle's spin. 8

2.3 Lowest order Feynman diagrams for $p\bar{p} \to e^+e^-$. 12

2.4 $\hat{\theta}$, the angle between the outgoing electron and the incoming quark in the rest frame of the electron pair. 13

2.5 Forward–backward asymmetry as a function of $\sin^2\theta_W$. The dotted curve shows the u–type asymmetry while the dashed curve shows the asymmetry for d–type quarks. The solid curve is the observed asymmetry for EHLQ 1 momentum distribution functions. 15

2.6 The Collins–Soper definition of the angle $\hat{\theta}$. The $\hat{z}$ axis bisects the proton and minus the antiproton directions. 17

3.1 An overhead view of the Fermilab accelerator complex. The fixed target beam lines are shown, as is the position of the B0 intersection region where the CDF detector is located. 20

3.2 The integrated luminosities delivered by the accelerator and recorded by the CDF detector. 23

one can derive a value for the "mixing angle", θ_W. This angle describes the mixing of the $SU(2)_L$ and $U(1)_Y$ sectors of the Standard Model, and is an integral parameter of the theory. If the Standard Model is correct, then the measured values of θ_W must be the same for all physical phenomena. Measurement of the mixing angle with many different processes, then, is an important test of the consistency of the model.

Chapter 2

Theory

By 1960, the phenomenology of the charged weak interactions was beginning to be understood, but there was no complete theory, like QED, for the weak interactions. It was clear, however, that both the weak and electromagnetic interactions share important properties: each uses a single coupling constant to describe a large number of physical phenomena, and both are mediated by spin-one fields. As early as 1957 Schwinger [7] suggested that the weak and electromagnetic forces were generated by an isospin triplet of fields; the two charged fields generated the weak interactions, while the neutral field was responsible for electromagnetism. This simple model ran into phenomenological trouble, but it is of historical importance as the first to suggest that the weak and electromagnetic interactions could be unified.

In 1961, Glashow [1] proposed a "partial symmetry" for the weak and electromagnetic interactions. In this model, weak interactions are described by two components of an isotopic spin group, $SU(2)_L$, which has coupling constant g and couples only to left-handed particles and right-handed antiparticles. The form of the $SU(2)_L$ interaction is determined by weak interaction phenomenology. The electromagnetic interaction is included by introducing a U(1) group with coupling constant g' which couples to hypercharge, in analogy with the Gell-Mann–Nishijima [8] model relating strangeness, baryon number, isospin, and charge in

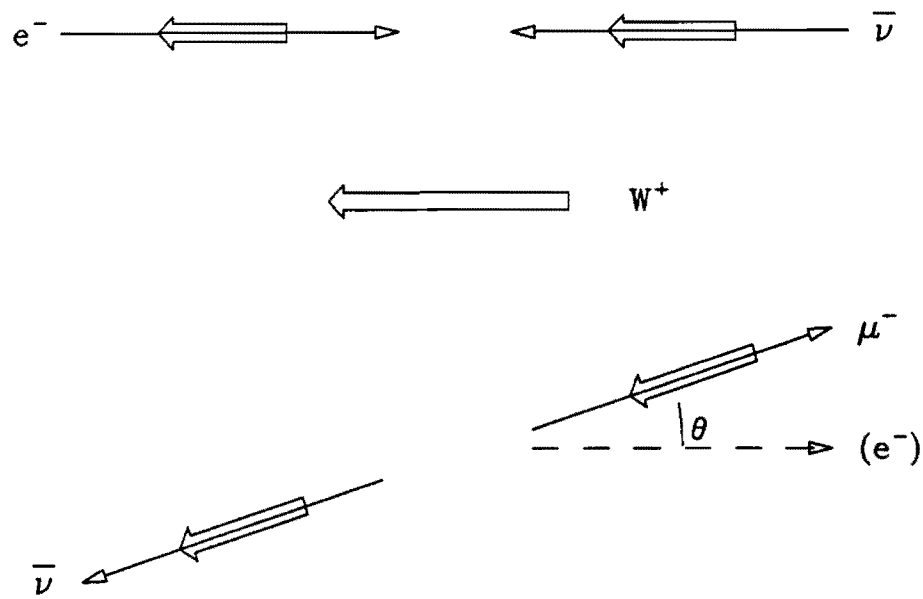

Figure 2.2: Momenta and spins in inverse muon decay, $e^-\bar{\nu}_e \to \mu^-\bar{\nu}_\mu$. A single arrow indicates the direction of a particle's momentum vector, while the double arrow shows the projection of the particle's spin.

inversion.

Assuming massless fermions, the angular distribution of the emitted muon in the inverse muon decay example is given by [11]

$$\frac{d\sigma}{d\cos\theta} = (1+\cos\theta)^2, \tag{2.15}$$

where θ is defined to be the angle between the incoming electron and outgoing muon in the rest frame of the W^-, as shown in Figure 2.2. A convenient quantity for characterizing the angular distribution is the forward–backward asymmetry, A_{FB}, defined by